Evidence of the Existence of Magnetism in Pristine VX_2 Monolayers (X = S, Se) and Their Strain-Induced Tunable Magnetic Properties

Yandong Ma, Ying Dai,* Meng Guo, Chengwang Niu, Yingtao Zhu, and Baibiao Huang

School of Physics, State Key Laboratory of Crystal Materials, Shandong University, Jinan 250100, People's Republic of China.

ABSTRACT

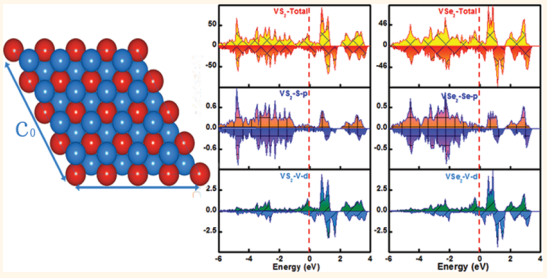

First-principles calculations are performed to study the electronic and magnetic properties of VX_2 monolayers (X = S, Se). Our results unveil that VX_2 monolayers exhibit exciting ferromagnetic behavior, offering evidence of the existence of magnetic behavior in pristine 2D monolayers. Furthermore, interestingly, both the magnetic moments and strength of magnetic coupling increase rapidly with increasing isotropic strain from −5% to 5% for VX_2 monolayers. It is proposed that the strain-dependent magnetic moment is related to the strong ionic−covalent bonds, while both the ferromagnetism and the variation in strength of magnetic coupling with strain arise from the combined effects of both through-bond and through-space interactions. These findings suggest a new route to facilitate the design of nanoelectronic devices for complementing graphene.

KEYWORDS: density functional theory · controllable magnetic · VS_2 monolayer · VSe_2 monolayer · strain

Graphene, a two-dimensional (2D) single layer of carbon atoms arranged in a honeycomb lattice, has been the focus of recent research efforts,[1−3] due to its unique zero-gap electronic structure and the massless Dirac Fermion behavior. The unusual electronic and structural properties make graphene a promising material for the next generation of faster and smaller electronic devices. Besides graphene, other 2D compounds such as BN, ZnO, transition metal oxides, and transition metal dichalcogenides (TMDs) are also of particular interest due to their unique properties that are useful for applications including a new generation of transistors, photoemitting devices, hydrogen storage, and spintronic devices.[4−12] In most of these existing pristine 2D materials no magnetic ordering is expected.[13−15] Fortunately, there are various alternative experimental approaches of magnetic modulation to induce magnetism, such as introducing transition metal atoms, point defects, and nonmetal element adsorption.[16−18]

However, for use in nanoelectronics, the magnetic coupling modulated by the conventional methods mentioned above in these nonmagnetic 2D materials is always somewhat rough as compared to the ideal requirement (stable and precision magnetic spin ordering) and, thus, is inconvenient to control in the actual application, which hampers the development of these materials in nanoelectronic devices. In addition, advanced applications often require materials with magnetic properties which can be deliberately tuned by external control parameters such as applied electric fields, elastic stress, or light.[19−21] In this respect, the acquisition of a 2D material, beyond the current 2D materials, with both precise and controllable spin ordering remains an important challenge.

In analogy to graphene, the 2D TMDs monolayer has attracted broad interest during recent years.[22−30] TMDs could occur in more than 40 different types,[31,32] depending on the combination of chalcogen (S, Se, or Te) and transition metal. Depending on the coordination and oxidation state of the metal atoms, TMDs can be metallic, semimetallic, or semiconducting.[31,32] This versatility makes it more intriguing if precise and controllable spin ordering can be obtained in these potential TMD monolayers. Very

* Address correspondence to daiy60@sina.com.

Received for review December 1, 2011 and accepted January 20, 2012.

Published online January 20, 2012
10.1021/nn204667z

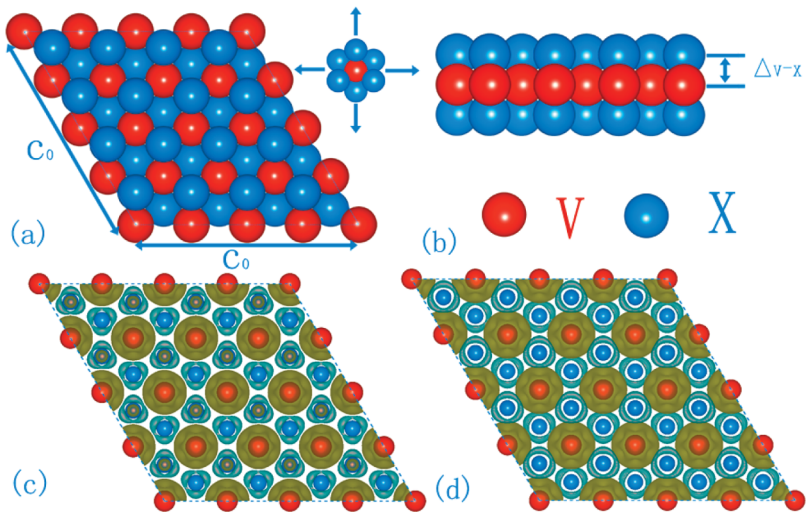

Figure 1. Geometric structures of VX_2 monolayers in top (a) and side (b) views. In the inset, we show that the strain is applied along zigzag and armchair directions. The spin-resolved charge density isosurface (isosurface value = 0.002 e/Å^3) of VS_2 (c) and VSe_2 (d) monolayers in ferromagnetic state. Yellow (blue) indicates the positive (negative) values.

recently, a new 2D TMD, a VS_2 monolayer, has been synthesized experimentally,[22,23] providing a potentially novel avenue for achieving promising functional materials for nanoelectronic applications. It was pointed out that the synthesis procedures are flexible for other 2D TMD monolayers, such as a VSe_2 monolayer.[23] Yet, it is known that, since the first discovery of bulk VS_2 in 1970, many difficulties hamper the scientist from investigating this material, resulting in the long term absence of systematic research work on VS_2.[22,33,34] Thus, for further development and applications, a systematic theoretical understanding of these monolayers would be highly desirable. Moreover, the complicated and versatile electronic structure of 2D TMD monolayers inspires us to believe that VS_2 and VSe_2 monolayers deserve specific attention as possible 2D materials with both precise and controllable magnetism.

In the present study, we systematically investigated the electronic and magnetic properties of VS_2 and VSe_2 monolayers, as well as the intercoupling between the strain and magnetic properties, by means of density functional theory calculations. It is shown that the pristine VS_2 and VSe_2 monolayers surprisingly exhibit magnetic ordering. More interestingly, the magnetic moments and the strength of magnetic coupling increase rapidly with increasing isotropic strain from −5% to 5% for VS_2 and VSe_2 monolayers. It is demonstrated that the strain-dependent magnetic moment is related to the strong ionic−covalent bonds, while both the ferromagnetism and the variation in strength of magnetic coupling with strain arise from the combined effects of both through-bond and through-space interactions. Motivated by these results, we propose and demonstrate a nanomechanical modulation of strain to sensitively enhance or quench the spin polarization of VS_2 and VSe_2 monolayers. Our work offers a new avenue for controllable and tunable spintronic devices.

TABLE 1. Calculated Lattice Constant (a), V−X Bond Length (d_{M-X}), Buckled Height between Two X Atom Planes (Δ_{X-X}), and Buckled Height between X and V Atom Planes (Δ_{V-X}) for Optimized MX_2 Monolayer

	a (Å)	d_{V-X} (Å)	Δ_{X-X} (Å)	Δ_{V-X} (Å)
VS_2	3.174	2.349	2.939	1.469
VSe_2	3.331	2.488	3.165	1.582

RESULTS AND DISCUSSION

For the convenience of our discussion, hereafter, the VS_2 and VSe_2 monolayer system is denoted by VX_2 monolayers (X = S, Se) for short. As shown in Figure 1, in such a monolayer, an intermediate layer of hexagonally arranged V atoms is sandwiched between two layers of X atoms, giving a trigonal prismatic arrangement. The optimized lattice parameters are listed in Table 1. Since the reduced dimensionality may sometimes result in magnetic behavior, we checked the possibility of spin-polarized ground states for pristine VX_2 monolayers, although it is the currently accepted view that no spontaneous magnetization can be expected in most 2D materials.[13−15] Based on our spin-polarized calculations, it is exciting that pristine VX_2 monolayers do exhibit magnetic ordering. For the VS_2 monolayers, the V atom possesses an ∼0.486 μ_B magnetic moment, while the X atom carries a small magnetic moment of ∼ −0.026 μ_B, and these values are 0.680 μ_B and −0.048 μ_B, respectively, for the VSe_2 case.

The existence of magnetic moment does not necessarily result in spin ordering. It thus is necessary to study the preferred magnetic coupling of these moments. Depending on the initial conditions of self-consistent calculations, two stable magnetic structures are obtained: one is ferromagnetic (FM), and the other is antiferromagnetic (AFM). Total energy calculations show the ground state to be FM in both cases, which

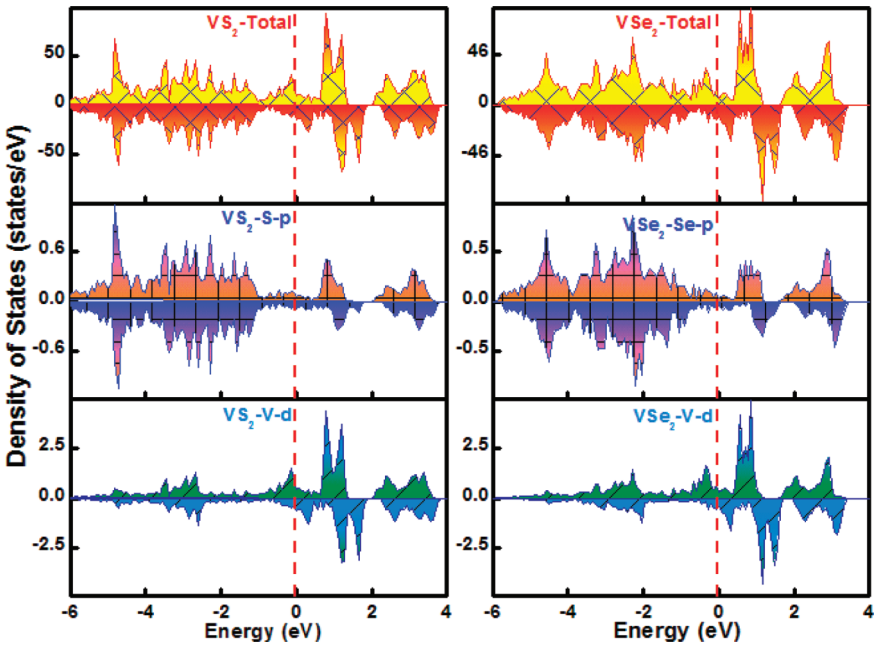

Figure 2. Total DOS and corresponding PDOS of VX_2 monolayers. The vertical dashed line represents the Fermi level.

lies 205 and 377 meV lower in energy than that of AFM for VS_2 and VSe_2 monolayers, respectively. Since the calculations are based on a supercell that consists of sixteen unit cells, the energy of the FM state for one unit cell composed of one V atom and two X atoms is 13 and 24 meV lower in energy than that of the AFM state, respectively, for VS_2 and VSe_2 monolayers. To drive the strength of the exchange coupling, we employ the Heisenberg model, $H = -J \sum_i \sigma_i \sigma_{i+1}$, where J is the exchange coupling parameter, and σ_i is the net spin induced by the ith vacancy. On the basis of this model, ΔE can be deduced as $E^{AFM} - E^{FM} = 2J|\sigma_i|^2$. Comparing this result with ΔE from *ab initio* calculations, a positive exchange coupling J = 26 meV (48 meV) is yielded in the VS_2 (VSe_2) system, indicating an appreciable magnetic coupling. It should be noted that the ferromagnetic interaction between the V atoms is a short-range order.

In order to understand in more detail the magnetic properties in the VX_2 monolayers, we plot the density of states (DOS) and the atomic site projected density (PDOS) in Figure 2. As Figure 2 illustrates, the VX_2 monolayers are metallic, which is consistent with the experimental results.[22] Moreover, it can be seen that the spin-up channel locates at a lower energy relative to the spin down channel, but both share similar distributions in reciprocal space. Examination of the PDOS of V and X atoms shows that V *d* states are relatively delocalized and hybridized with X *p* states, indicating some covalent-like component of the V−X bond. To visualize the distribution of spins on VX_2 monolayers, the isosurface spin density is plotted in Figure 1c and d. It is evident that the magnetism is mainly contributed by the V atoms, while all of the X atoms have little contribution to the total moment, which is consistent with the results obtained from PDOS.

According to the analysis above, FM behavior has been predicated theoretically in pristine 2D materials. Yet, advanced applications often require materials with magnetic properties which can be deliberately modulated in a well-controlled manner, which is central to actual applications.[19−21] On the other hand, strain effect is always important in nanosystems. Previous studies indicated that the spin polarization exhibits remarkable strain dependence in topologically fluorinated BN nanotubes, and increasing local strain can enhance the relatively weak FM order.[35,36] Moreover, the half-fluorinated BN and GaN sheets can exhibit intriguing magnetic transitions between ferromagnetism and antiferromagnetism by applying strain.[17] Motivated by these results, we guess that a nanomechanical modulation of strain can sensitively enhance or quench the spin polarization of VX_2 monolayers. Note that the VX_2 monolayers are two-dimensional materials; due to the limited size along the direction perpendicular to the plane of the layers, strain exerted along this direction would be hard to modulate in a well controlled manner in experiments. Therefore, following previous work,[17] we only focus on the strain applied along the direction parallel to the plane of the layers. Here, we investigate the strain dependence of magnetic properties in VX_2 monolayers by varying the isotropic strain from −5% to 5%, by which all crystal symmetries and the overall honeycomb-like structure are maintained. The tensile or compression strain is uniformly applied along both zigzag and armchair directions as shown in the inset of

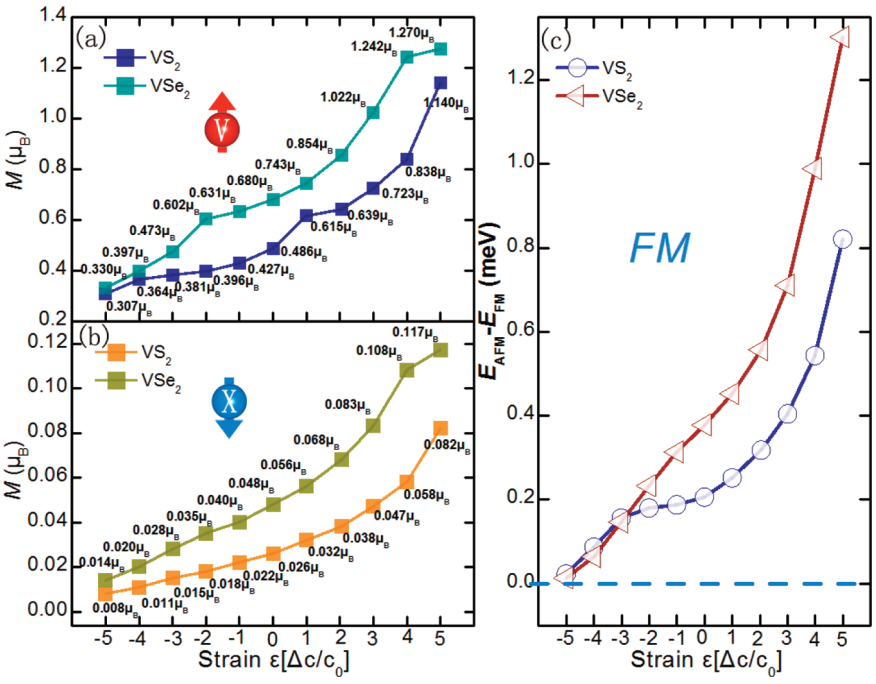

Figure 3. Strain dependence of the magnetic moment per V atom M_V (a), the magnetic moment per X atom M_X (b), and the energy difference between FM and AFM order (c) of VX_2 monolayers.

Figure 1a. The isotropic strain is defined as $\varepsilon = \Delta c/c_0$, where the lattice constants of the unstrained and strained supercell are equal to c_0 and $c = \Delta c + c_0$, respectively.[37,38] The stretching or compressing of the VX_2 monolayers is achieved by first elongating the optimized lattice constant c_0 to $c = \Delta c + c_0$ and uniformly expanding the atomic structure obtained from the previous optimization. Subsequently, the atomic structure is reoptimized and the corresponding energy is calculated with the elongated lattice constant fixed.

Figure 3 shows the variation in the magnetic moment per V atom (M_V) and the magnetic moment per X atom (M_X) of the VX_2 monolayers with strain. It is found that the magnetic moments M_V and M_X increase monotonically with increasing isotropic strain from −5% to 5% for VX_2 monolayers. More surprisingly, for the VX_2 systems under tensile stress, it is shown that the magnetic moment M_V of the strained VX_2 monolayers with ε = 5% increases up to 1.140 μ_B and 1.270 μ_B, an approximately 187% and 235% enhancement over the undeformed level for the VS_2 and VSe_2 monolayers, respectively. The magnetic moment M_X of the VS_2 and VSe_2 monolayers with ε = 5% also shows a 315% and 244% enhancement, respectively, over their undeformed levels. However, for the compressive stress on the VX_2 monolayers, with increasing compression, the magnetic moments M_V and M_X rapidly decrease. Yet, at 5% compression, the magnetic moment M_V is calculated to be 0.307 μ_B and 0.330 μ_B, which are still analogous with that of the BN nanotubes with topological fluorine adsorption reported in ref 39. In a word, the spin polarization in the VX_2 monolayers is robust within a wide range of strain. On the other hand, with increasing compression, the magnetic moment M_S (M_{Se}) is rapidly almost quenched, from 0.026 μ_B (0.048 μ_B) in the undeformed levels to 0.008 μ_B (0.014 μ_B) in the strained structures with $\varepsilon = -5\%$, indicating that the magnetic coupling under such conditions is almost quenched which we will discuss in detail in the following. Moreover, for application in nanoelectronics, 2D nanoscale magnets with FM spin ordering are more desirable. This requires FM coupling among the polarized electron spins in nanostructures. So we investigate the strain dependence of the spin ordering in VX_2 monolayers by varying the strain from −5% to 5%. The corresponding energy difference ΔE ($\Delta E = E_{AFM} - E_{FM}$) of VX_2 as a function of strain is illustrated in Figure 3, where substantial energy difference ΔE increases efficiently with higher tension and the FM state is always more stable than the AFM state for VX_2 monolayers under tensile stress, while the FM ordering is weakened for compression stress on VX_2 monolayers. Accordingly, the exchange coupling can be efficiently enhanced or quenched with increasing or decreasing strain. Therefore, for the VX_2 monolayers under stress, the interaction between the moments keeps FM coupling independent of the strain (as shown in Figure 3). Furthermore, the FM coupling is strongly more stable than the AFM order, which reveals that the FM spin ordering in VX_2 monolayers is robust within a large range of strain. The rapid variation of spin polarization in VX_2 monolayers under strain may be useful for applications in nanodevices, such as a mechanical switch for spin-polarized transport.

Explanation of this interesting change of the spin polarization with strain is sought in the particular interactions between the V and X atoms. For VX_2 monolayers, the magnetic moment can be determined by the competition of two distinct interactions between the V and X atoms: (a) ionic bonding interaction and (b) covalent bonding interaction. Evidently, both the ionic bonding interaction and covalent bonding interaction depend sensitively on strain, due to the fact that the distance between two neighboring atoms (d_{V-X}) increases with increasing tensile strain or decreasing compression strain, and the elongating of the d_{V-X} results in reduction in the covalent bonding interaction and enhancement in the ionic bonding interaction. Accordingly, the relative increase of the ionic composition of the interaction between the V and X atoms leads to a slight increase in the unpaired electrons accumulated on the V and X atoms, thus giving rise to the interesting variation in the magnetic moment of the VX_2 monolayers with strain.

On the other hand, the variation in energy difference ΔE of the VX_2 monolayer with strain can be understood from the aspect of its magnetic mechanism. From the above discussion, it is shown that the coupling between the spins in the VX_2 monolayer is FM. It seems that ferromagnetism of the VX_2 monolayer without strain arises from the effect of through-bond spin polarization.[40,41] For the through-bond spin polarization, it is defined that an atom with an up-spin (down-spin) density induces a down-spin (up-spin) density on the adjacent atom directly bonded to it. Provided that *b*(*i*) and *b*(*j*) represent the *b* atoms at sites *i* and *j*, respectively, the through-bond spin polarization takes place along each *b*(*i*)-(*a*-*b*)n-*a*-*b*(*j*) (*n* = 0, 1, 2,...) path. For all *b*-*b* couplings, each *b*(*i*)-(*a*-*b*)n-*a*-*b*(*j*) path consists of an even number of *a*-*b* bonds. Consequently, the through-bond spin polarization ferromagnetically couples the spins of the VX_2 monolayer. As expected from the mechanism of through-bond spin polarization, the up-spin and down-spin densities occur on the V and X atoms, respectively, which is consistent with the isosurface spin density plotted in Figure 1. Yet, based on this mechanism, elongation of d_{V-X} induced by increasing the tensile strain (or decreasing the compression strain) would result in the reduction in the spin coupling, namely, the decrease in energy difference ΔE, which is in contradiction to the present results. These reveal that the through-bond spin polarization alone is not credible in these systems. Here, we employ the mechanism which was proposed in our previous work[17,42] to understand the magnetism in these VX_2 systems. In this mechanism, we find that the magnetism can be determined by the competition of two distinct interactions: (a) through-bond interaction and (b) through-space interaction. For the through-space interaction, it is defined that a *b* atom with an up-spin (down-spin) density induces a down-spin (up-spin) density on the nearest-neighboring *b* atom directly, without mediation by an *a* atom. Provided that *b*(*i*) and *b*(*j*) represent the *b* atoms at sites *i* and *j*, respectively, the through-space interaction takes place along each *b*(*i*)-(*b*)n-*b*(*j*) (*n* = 0, 1, 2,...) path. As a result, the through-space interaction antiferromagnetically couples the spins of the VX_2 monolayer. Based on this combined mechanism, the variation in energy difference ΔE as a function of strain can be easily understood. As a consequence of the fact that both through-bond interaction and through-space interaction depend sensitively on d_{V-X}, elongation of d_{V-X} induced by increasing the tensile strain (or decreasing the compression strain) leads to the reduction in both through-bond interaction and through-space interaction. However, the through-space interaction compared to the through-bond interaction is greatly reduced with increasing tensile strain (or decreasing compression strain), resulting in the relative increase of the through-bond interaction, which can give a good explanation of the fact that energy difference ΔE increases monotonically with increasing isotropic strain from −5% to 5% for VX_2 systems. Besides, given the success in explaining the strain effects on VX_2 monolayers, we can also verify that the magnetism of VX_2 monolayers arises from the combined effects of both through-bond and through-space interactions and, of course, the interactions between the magnetic moments are mainly determined by the effect of through-bond interaction, resulting in FM VX_2 monolayers. The particular properties of the VX_2 monolayers have the potential for wider applications of 2D-based materials and devices.

CONCLUSION

Systematic first-principles calculations are carried out to understand the electronic and magnetic properties of VX_2 monolayers. Our findings can be summarized into four main points:

(1) It is demonstrated that pristine VS_2 and VSe_2 monolayers exhibit exciting ferromagnetic behavior, offering evidence of the existence of magnetic behavior for pristine 2D monolayers.

(2) Magnetic moments and the energy difference ΔE increase rapidly with increasing isotropic strain from −5% to 5% for VX_2 monolayers. Accordingly, nanomechanical modulation of strain can sensitively enhance or quench the spin polarization and the strength of the exchange coupling of VX_2 monolayers, which may find application in nanodevices, such as a mechanical switch for spin-polarized transport.

(3) Explanation of the interesting change of the spin polarization with strain is sought in the particular ionic−covalent interactions between the V and X atoms. The increase in the ionic composition of the interaction between the V and X atoms induced by strain leads to a

slight increase in the unpaired electrons accumulated on the V and X atoms, thus giving rise to the interesting variation in magnetic moment.

(4) It is demonstrated that the ferromagnetism of VX_2 monolayers arises from the combined effects of both through-bond and through-space interactions. Both through-bond interaction and through-space interaction depend sensitively on the strain. According to this combined mechanism, the variation in energy difference ΔE with strain can be easily understood.

The interesting and large tunability of the ferromagnetic properties of VS_2 and VSe_2 monolayers may present hopeful candidates for application in nanodevices. It should be noted that it will be interesting to observe the ferromagnetism in VX_2 (X = S, Se) monolayers in advanced experiments, and defects/local strains which would affect the magnetic properties usually present in VX_2 (X = S, Se) monolayers during growth in actual conditions, so the more comprehensive factors may be discussed in further work. We hope that the present study will stimulate further experimental effort in this field.

METHODS

All of our calculations, including geometry relaxation and electronic structure calculation, are based on the spin-polarized density functional theory (DFT) using generalized gradient approximation (GGA)[43] for exchange-correlation potential. The Perdew−Burke−Ernzerhof (PBE) functional was used for GGA as implemented in the Vienna *ab initio* Simulation Package (VASP).[44,45] For the geometric and electronic structural calculations, a supercell consisting of 4×4 unit cells of VS_2 or VSe_2 monolayers is employed. A vacuum layer of 17 Å is adopted in the direction normal to the interface, representing the isolated slab boundary condition. The Brillouin zone is represented by the set of $6 \times 6 \times 1$ k-points[46] for the geometry optimizations and by that of $8 \times 8 \times 1$ k-points for the static total energy calculations. The energy cutoffs, convergence in energy, and force are set to 400 eV, 1×10^{-5} eV, and 0.02 eV/Å, respectively. Test calculations with larger energy cutoffs ensure that the results are fully converged. It is well-known that the GGA would underestimate the energy gap due to a well-known shortcoming of DFT. However, the occupied states and the dispersion of the band and the characters of the band structures as well as the relative variation are expected to be qualitatively reasonable and reliable. Besides, almost all of the early studies of the 2D TMD monolayer systems were based on GGA,[8,22,24,47−49] neglecting the GGA+U method, and for VX_2 monolayers, they are of metallic character without an energy gap. Thus, for convenient comparison with the previous work, we employ the GGA method in the present work.

Acknowledgment. This work is supported by the National Basic Research Program of China (973 program, 2007CB613302), National Science Foundation of China under Grants 11174180 and 20973102, and the Natural Science Foundation of Shandong Province under Grant No. ZR2011AM009.

REFERENCES AND NOTES

1. Novoselov, K. S.; Geim, A. K. S.; Morozov, V.; Jiang, D.; Zhang, Y.; Dubonos, S. V.; Grigorieva, I. V.; Firsov, A. A. Electric Field Effect in Atomically Thin Carbon Films. *Science* **2004**, *306*, 666–669.
2. Novoselov, K. S.; McCann, E.; Morozov, S. V.; Falko, V. I.; Katsnelson, M. I.; Zeitler, U.; Jiang, D.; Schedin, F.; Geim, A. K. Unconventional Quantum Hall Effect and Berry's Phase of 2_π in Bilayer Graphene. *Nat. Phys.* **2006**, *2*, 177–180.
3. Zhang, Y. B.; Tan, Y. W.; Stormer, H. L.; Kim, P. Experimental Observation of the Quantum Hall Effect and Berry's Phase in Graphene. *Nature* **2005**, *438*, 201–204.
4. Radisavljevic, B.; Radenovic, A.; Brivio, J.; Giacometti, V.; Kis, A. Single-Layer MoS_2 Transistors. *Nat. Nanotechnol.* **2011**, *6*, 147–150.
5. Ma, Y. D.; Dai, Y.; Wei, W.; Niu, C. N.; Yu, L.; Huang, B. B. First-Principles Study of the Graphene@$MoSe_2$ Heterobilayers. *J. Phys. Chem. C* **2011**, *115*, 20237–20241.
6. Splendiani, A.; Sun, L.; Zhang, Y.; Kim, T.; Li, J.; Chim, C.-Y.; Galli, G.; Wang, F. Emerging Photoluminescence in Monolayer MoS_2. *Nano Lett.* **2010**, *10*, 1271–1275.
7. Seayad, A. M.; Antonelli, D. M. Recent Advances in Hydrogen Storage in Metal-Containing Inorganic Nanostructures and Related Materials. *Adv. Mater.* **2004**, *16*, 765–777.
8. Ma, Y. D.; Dai, Y.; Guo, M.; Niu, C. N.; Lu, J. B.; Huang, B. B. Electronic and Magnetic Properties of Perfect, Vacancy-Doped, and Nonmetal Adsorbed $MoSe_2$, $MoTe_2$ and WS_2 Monolayers. *Phys. Chem. Chem. Phys.* **2011**, *13*, 15546–15553.
9. Tang, Q.; Li, F. Y.; Zhou, Z.; Chen, Z. F. Versatile Electronic and Magnetic Properties of Corrugated V_2O_5 Two-Dimensional Crystal and Its Derived One-Dimensional Nanoribbons: A Computational Exploration. *J. Phys. Chem. C* **2011**, *115*, 11983–11990.
10. Tang, Q.; Cui, Y.; Li, Y. F.; Zhou, Z.; Chen, Z. F. How Do Surface and Edge Effects Alter the Electronic Properties of GaN Nanoribbons? *J. Phys. Chem. C* **2011**, *115*, 1724–1731.
11. Li, Y. F.; Li, F. Y.; Zhou, Z.; Chen, Z. F. SiC_2 Silagraphene and Its One-Dimensional Derivatives: Where Planar Tetracoordinate Silicon Happens. *J. Am. Chem. Soc.* **2011**, *133*, 900–908.
12. Tang, Q.; Cui, Y.; Li, Y. F.; Zhou, Z.; Chen, Y. S.; Chen, Z. F. Tuning Electronic and Magnetic Properties of Wurtzite ZnO Nanosheets by Surface Hydrogenation. *ACS Appl. Mater. Interfaces* **2010**, *2*, 2442–2447.
13. Zhou, J.; Sun, Q. Magnetism of Phthalocyanine-Based Organometallic Single Porous Sheet. *J. Am. Chem. Soc.* **2011**, *133*, 15113–15119.
14. Abel, M.; Clair, S.; Ourdjini, O.; Mossoyan, M.; Porte, L. Single Layer of Polymeric Fe-Phthalocyanine: An Organometallic Sheet on Metal and Thin Insulating Film. *J. Am. Chem. Soc.* **2011**, *133*, 1203–1205.
15. Shi, Z. L.; Liu, J.; Lin, T.; Xia, F.; Liu, P. N.; Lin, N. Thermodynamics and Selectivity of Two-Dimensional Metallo-supramolecular Self-Assembly Resolved at Molecular Scale. *J. Am. Chem. Soc.* **2011**, *133*, 6150–6153.
16. Krasheninnikov, A. V.; Lehtinen, P. O.; Foster, A. S.; Pyykko, P.; Nieminen, R. M. Embedding Transition-Metal Atoms in Graphene: Structure, Bonding, and Magnetism. *Phys. Rev. Lett.* **2009**, *102*, 126807–126810.
17. Ma, Y. D.; Dai, Y.; Guo, M.; Niu, C. N.; Yu, L.; Huang, B. B. Strain-Induced Magnetic Transitions in Half-Fluorinated Single Layers of BN, GaN and Graphene. *Nanoscale* **2011**, *3*, 2301–2306.
18. Crvenka, J. S.; Katsnelson, M. I.; Flipse, C. F. J. Room-Temperature Ferromagnetism in Graphite Driven by Two-Dimensional Networks of Point Defects. *Nat. Phys.* **2009**, *5*, 840–844.
19. Chiba, D.; Yamanouchi, M.; Matsukura, F.; Ohno, H. Electrical Manipulation of Magnetization Reversal in a Ferromagnetic Semiconductor. *Science* **2003**, *301*, 943–945.
20. Bihler, C.; Althammer, M.; Brandlmaier, A.; Geprags, S.; Weiler, M.; Opel, M.; Schoch, W.; Limmer, W.; Gross, R.;

Brandt, M. S.; et al. $Ga_{1-x}Mn_xAs$/Piezoelectric Actuator Hybrids: A Model System for Magnetoelastic Magnetization Manipulation. *Phys. Rev. B: Condens. Matter Mater. Phys.* **2008**, *78*, 045203–045216.
21. Tanaka, H.; Zhang, J.; Kawai, T. Giant Electric Field Modulation of Double Exchange Ferromagnetism at Room Temperature in the Perovskite Manganite/Titanate p-n Junction. *Phys. Rev. Lett.* **2001**, *88*, 027204–027207.
22. Feng, J.; Sun, X.; Wu, C.; Peng, L.; Lin, C.; Hu, S.; Yang, J.; Xie, Y. Metallic Few-Layered VS_2 Ultrathin Nanosheets: High Two-Dimensional Conductivity for In-Plane Supercapacitors. *J. Am. Chem. Soc.* **2011**, *133*, 17832–17838.
23. Coleman, J. N.; Lotya, M.; O'Neill, A.; Bergin, S. D.; King, P. J.; Khan, U.; Young, K.; Gaucher, A.; De, S.; Smith, R. J.; Shvets, I. V.; et al. Two-Dimensional Nanosheets Produced by Liquid Exfoliation of Layered Materials. *Science* **2011**, *331*, 568–571.
24. He, J.; Wu, K.; Sa, R.; Li, Q.; Wei, Y. Magnetic Properties of Nonmetal Atoms Absorbed MoS_2 Monolayers. *Appl. Phys. Lett.* **2010**, *96*, 082504–082506.
25. Mak, K. F.; Lee, C.; Hone, J.; Shan, J.; Heinz, T. F. Atomically Thin MoS_2: A New Direct-Gap Semiconductor. *Phys. Rev. Lett.* **2010**, *105*, 136805–136808.
26. Splendiani, A.; Sun, L.; Zhang, Y.; Li, T.; Kim, J.; Chim, C.; Galli, G.; Wang, F. Emerging Photoluminescence in Monolayer MoS_2. *Nano Lett.* **2010**, *10*, 1271–1275.
27. Shahar, C.; Levi, R.; Cohen, S. R.; Tenne, R. Gold Nanoparticles as Surface Defect Probes for WS_2 Nanostructures. *J. Phys. Chem. Lett.* **2010**, *1*, 540–544.
28. Castellanos-Gomez, A.; Agrat, N.; Rubio-Bollinger, G. Optical Identification of Atomically Thin Dichalcogenide Crystals. *Appl. Phys. Lett.* **2010**, *96*, 213116–213118.
29. Novoselov, K.; Jiang, D.; Schedin, F.; Booth, T.; Khotkevich, V.; Morozov, S.; Geim, A. Two-Dimensional Atomic Crystals. *Proc. Natl. Acad. Sci. U.S.A.* **2005**, *102*, 10451–10453.
30. Li, Y. F.; Zhou, Z.; Zhang, S. B.; Chen, Z. F. MoS_2 Nanoribbons: High Stability and Unusual Electronic and Magnetic Properties. *J. Am. Chem. Soc.* **2008**, *130*, 16739–16744.
31. Marseglia, E. A. Transition Metal Dichalcogenides and Their Intercalates. *Int. Rev. Phys. Chem.* **1983**, *3*, 177–216.
32. Wilson, J. A.; Yoffe, A. D. The Transition Metal Dichalcogenides Discussion and Interpretation of the Observed Optical, Electrical and Structural Properties. *Adv. Phys.* **1969**, *18*, 193–335.
33. Murphy, D. W.; Cros, C.; Salvo, F. J. D.; Waszczak, J. V. Preparation and Properties of Li_xVS_2 ($0 \leq x \leq 1$). *Inorg. Chem.* **1977**, *16*, 3027–3031.
34. Therese, H. A.; Rocker, F.; Reiber, A.; Li, J.; Stepputat, M.; Glasser, G.; Kolb, U.; Tremel, W. VS_2 Nanotubes Containing Organic-Amine Templates from the NT-VO_x Precursors and Reversible Copper Intercalation in NT-VS_2. *Angew. Chem., Int. Ed.* **2005**, *44*, 262–265.
35. Li, F.; Zhu, Z.; Yao, X.; Lu, G. Fluorination-Induced Magnetism in Boron Nitride Nanotubes from Ab Initio Calculations. *Appl. Phys. Lett.* **2008**, *92*, 102515–102517.
36. Zhou, J.; Wang, Q.; Sun, Q.; Jena, P. Electronic and Magnetic Properties of a BN Sheet Decorated with Hydrogen and Fluorine. *Phys. Rev. B* **2010**, *81*, 085442–085448.
37. Choi, S.-M.; Jhi, S.-H.; Son, Y.-W. Effects of Strain on Electronic Properties of Graphene. *Phys. Rev. B* **2010**, *81*, 081407–085410.
38. Zhou, M.; Lu, Y. H.; Zhang, C.; Feng, Y. P. Strain Effects on Hydrogen Storage Capability of Metal-Decorated Graphene: A First-Principles Study. *Appl. Phys. Lett.* **2010**, *97*, 103109–103112.
39. Zhang, Z. H.; Guo, W. Tunable Ferromagnetic Spin Ordering in Boron Nitride Nanotubes with Topological Fluorine Adsorption. *J. Am. Chem. Soc.* **2009**, *131*, 6874–6879.
40. Jin, H.; Dai, Y.; Huang, B. B.; Whangbo, M.-H. Ferromagnetism of Undoped GaN Mediated by Through-Bond Spin Polarization Between Nitrogen Dangling Bonds. *Appl. Phys. Lett.* **2009**, *94*, 162505–162507.
41. Yoshizawa, K.; Kuga, T.; Sato, T.; Hatanaka, M.; Tanaka, T.; Yamabe, T. Through-Bond and Through-Space Interactions of Organic Radicals Coupled by *m*-Phenylene. *Bull. Chem. Soc. Jpn.* **1996**, *69*, 3443–3450.
42. Ma, Y. D.; Dai, Y.; Guo, M.; Niu, C. N.; Yu, L.; Huang, B. B. Magnetic Properties of the Semifluorinated and Semihydrogenated 2D Sheets of Group-IV and III-V Binary Compounds. *Appl. Surf. Sci.* **2011**, *257*, 7845–7850.
43. Perdew, J. P.; Burke, K.; Ernzerhof, M. Generalized Gradient Approximation Made Simple. *Phys. Rev. Lett.* **1996**, *77*, 3865–3868.
44. Kresse, G.; Furthmuller, J. Efficient Iterative Schemes for Ab Initio Total-Energy Calculations Using a Plane-Wave Basis Set. *Phys. Rev. B* **1996**, *54*, 11169–11186.
45. Kresse, G.; Joubert, J. From Ultrasoft Pseudopotentials to the Projector Augmented-Wave Method. *Phys. Rev. B* **1999**, *59*, 1758–1775.
46. Monkhorst, H. J.; Pack, J. D. Special Points for Brillouin-Zone Integrations. *Phys. Rev. B* **1976**, *13*, 5188–5192.
47. Lebègue, S.; Eriksson, O. Electronic Structure of Two-Dimensional Crystals from Ab Initio Theory. *Phys. Rev. B* **2009**, *79*, 115409–115412.
48. Liu, B.; Han, Y. H.; Gao, C. X.; Ma, Y. Z.; Peng, G.; Wu, B. J.; Liu, C. L.; Wang, Y.; Hu, T. G.; Cui, X. Y.; et al. Pressure Induced Semiconductor-Semimetal Transition in WSe_2. *J. Phys. Chem. C* **2010**, *114*, 14251–14254.
49. Zhu, Z. Y.; Cheng, Y. C.; Schwingenschlögl, U. Giant Spin-Orbit-Induced Spin Splitting in Two-Dimensional Transition-Metal Dichalcogenide Semiconductors. *Phys. Rev. B* **2009**, *84*, 153402–153406.